Electronic Supplementrary Information

Solution processed Gold Nanostar/Polydimethylsiloxane Flexible Substrates for Plasmonic Sensing

Amane Shiohara[†], Judith Langer[†], Lakshminarayana Polavarapu[†] and Luis M Liz-Marzán[†‡*]

[†]CIC biomGUNE, Paseo de Miramón 182, 20009 Donostia-San Sebastián, Spain

[‡]Ikerbasque, Basque Foundation for Science, 48011 Bilbao, Spain

* Corresponding author e-mail: llizmarzan@cicbiomagune.es

Synthesis of PVP coated Au nanostars

PVP coated Au nanostar synthesis was performed as previously reported.[16] Briefly, 820 μL of a 50 mM $HAuCl_4$ aqueous solution was mixed with 150 mL of 10 mM PVP (MW 10,000) solution in DMF. 723μL of PVP-coated Au seed (d = 15 nm, [Au^0] = 2.48 mM) in ethanol was added under continuous stirring at room temperature. Within 20 min, the color of the solution changed from pink to dark purple or dark blue, indicating the formation of Au nanostars. The nanostars were purified by centrifugation for 3 times with a speed of 4500 rpm and finally redispersed in ethanol.

Table S1. Average values of core size, tip length and aspect ratio, plasmon peak position, LSPR shift per RIU, LSPR band full width at half maximum (FWHM), and figure of merit (FOM) for three Au nanostar samples in aqueous solution.

	Average core size (nm)	Average tip length (nm) (aspect ratio)	Plasmon Peak (nm)	RIU	FWHM	FOM
Ag 10μM	30.03	15.34±7.3(1.1)	558	125.7	92.88	1.35
Ag 20μM	29.20	18.11± 8.5(1.7)	685	284.1	147.16	1.93
Ag 50μM	29.27	20.51± 5.7(2.4)	845	470.9	348.39	1.35

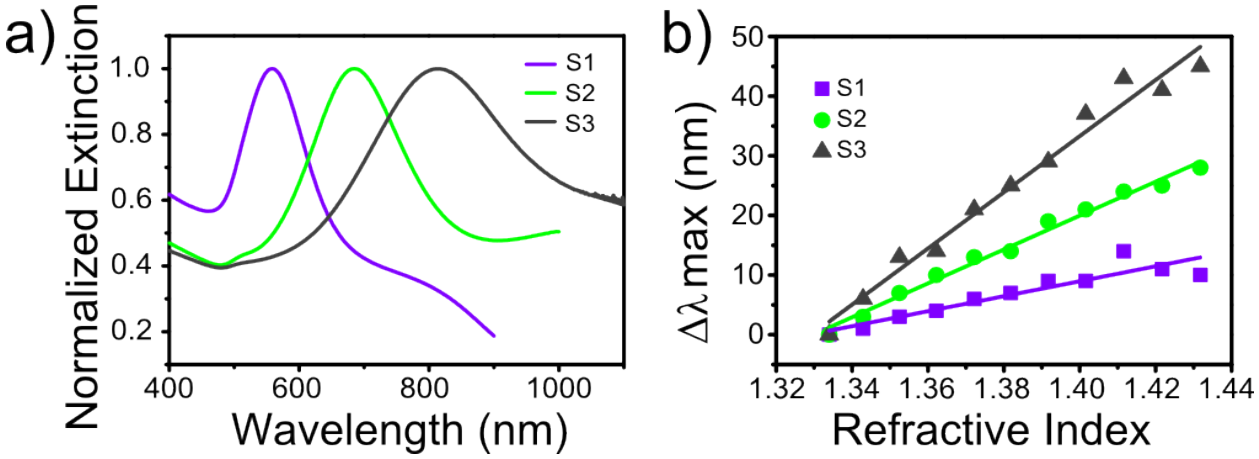

Figure S1: a) Extinction spectra of samples S1, S2, and S3 in water solution which are used to measure RI sensitivity. b) LSPR shift versus RI for samples S1, S2 and S3 in solution. The lines are linear fits to the data.

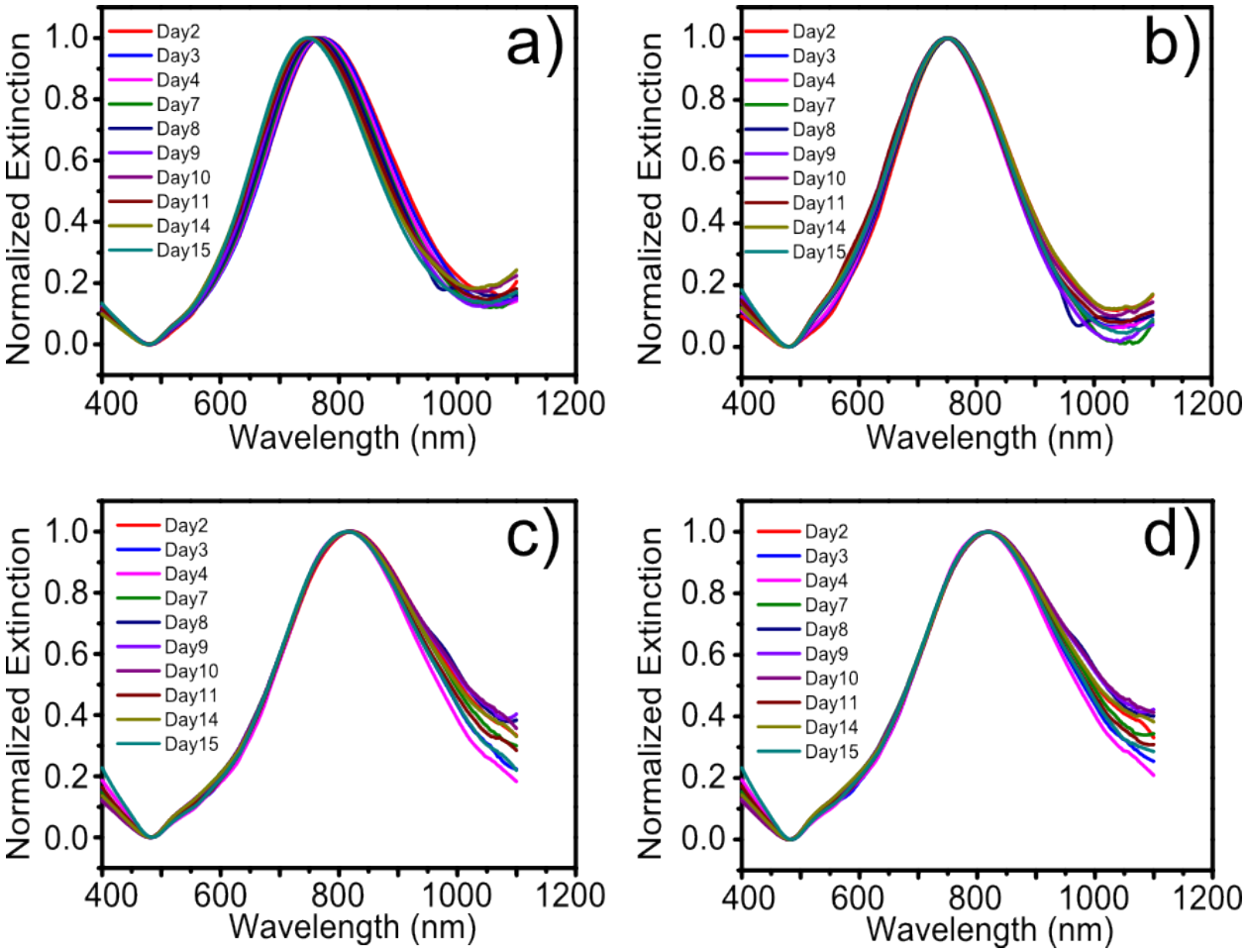

Figure S2: (a,b) Extinction spectra of PDMS/AuNS stored in the air (a) and under nitrogen (b) from day 2 to day 15. The spectra were measured immersing the PDMS strip in water. (c,d) Extinction spectra of PDMS/AuNS coated with ATP stored in the air (a) and under nitrogen (b) from day 2 to day 15. The spectra were measured immersing the PDMS strip in ethanol.

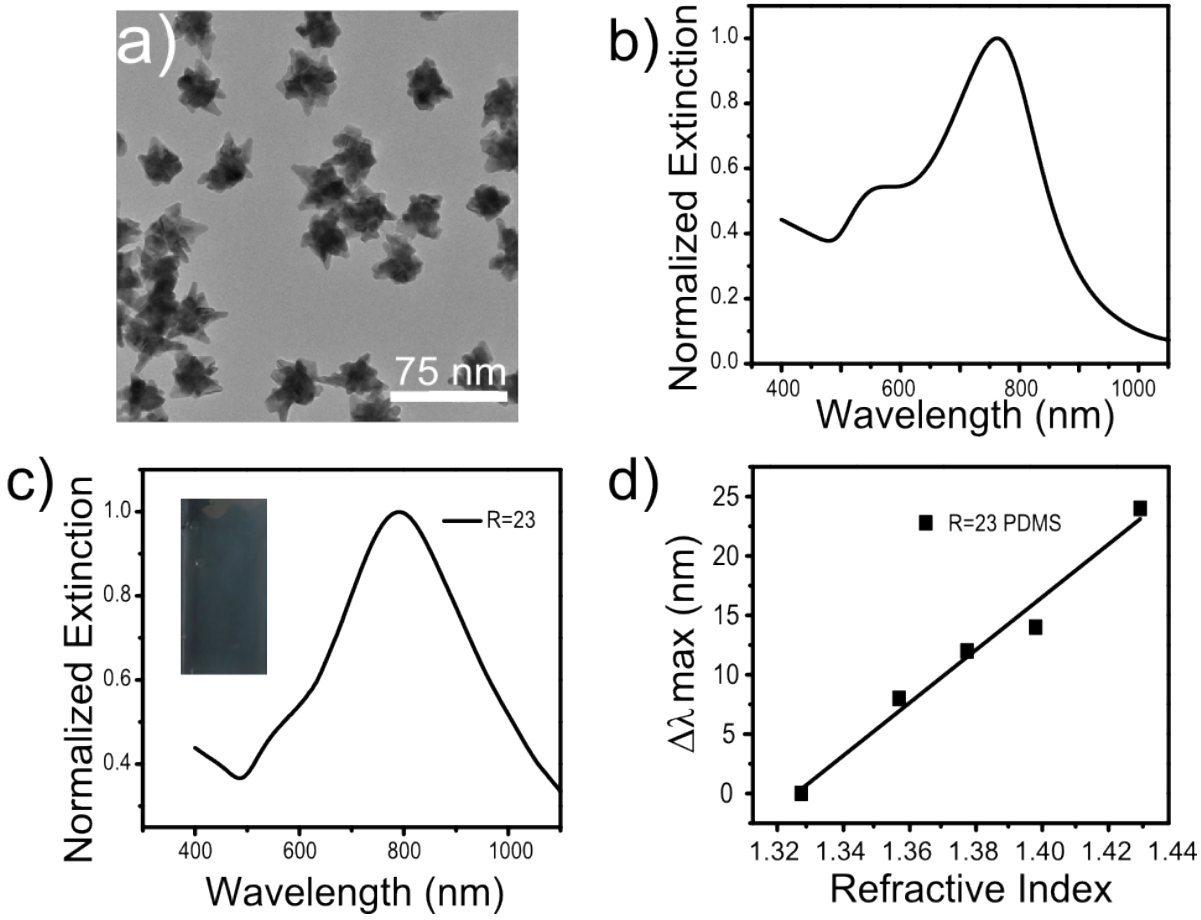

Figure S3: a) TEM image of PVP coated Au nanostars. b) Extinction spectrum of PVP coated Au nanostars in water. c) Extinction spectra of PVP coated Au nanostars adsorbed on a PDMS film, which was immersed in water. The inset shows a photograph of the film. d) LSPR shift versus refractive index for the PVP coated Au nanostars on PDMS film. The line is a linear fit to the data.

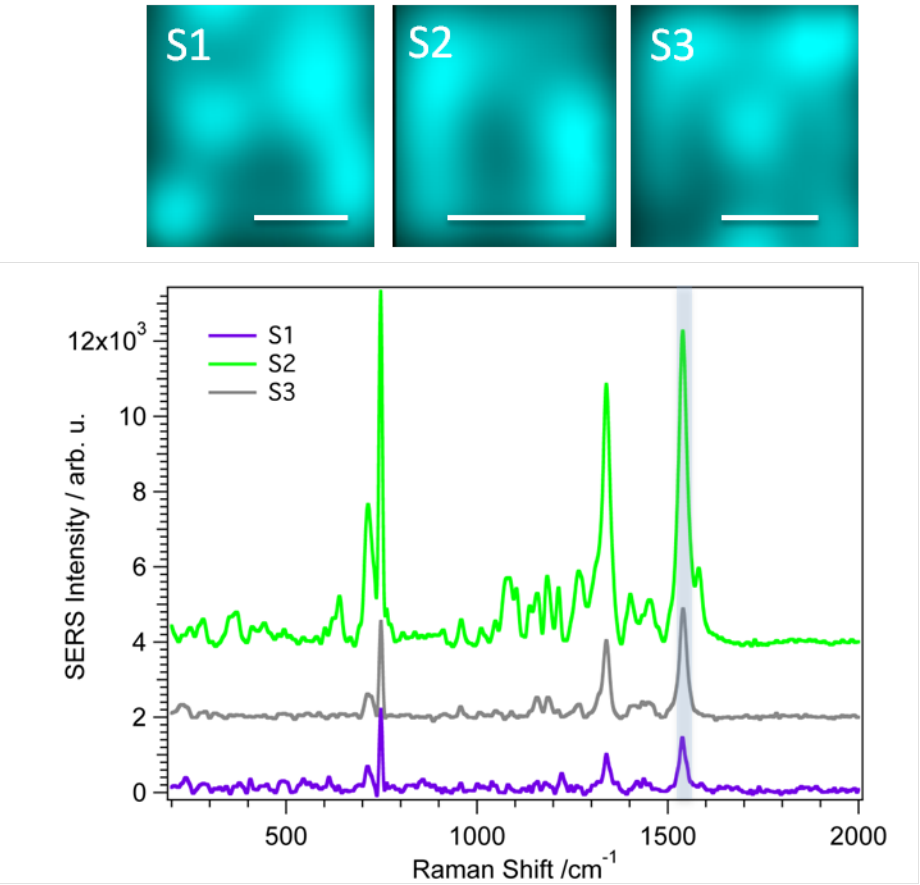

Figure S4: (a) SERS spectra of astra blue ([AB] = 10^{-7} M) on PDMS films covered with nanostars of different aspect ratios: S1 (1.1), S2 (1.7) and S3 (2.4). The spectra are background corrected and offsets were applied to improve data presentation. SERS maps over large areas were generated for the characteristic vibration of 1585 cm^{-1}, corresponding to the aromatic ring mode. The white bar on the maps corresponds to a scanning distance of 10 µm.

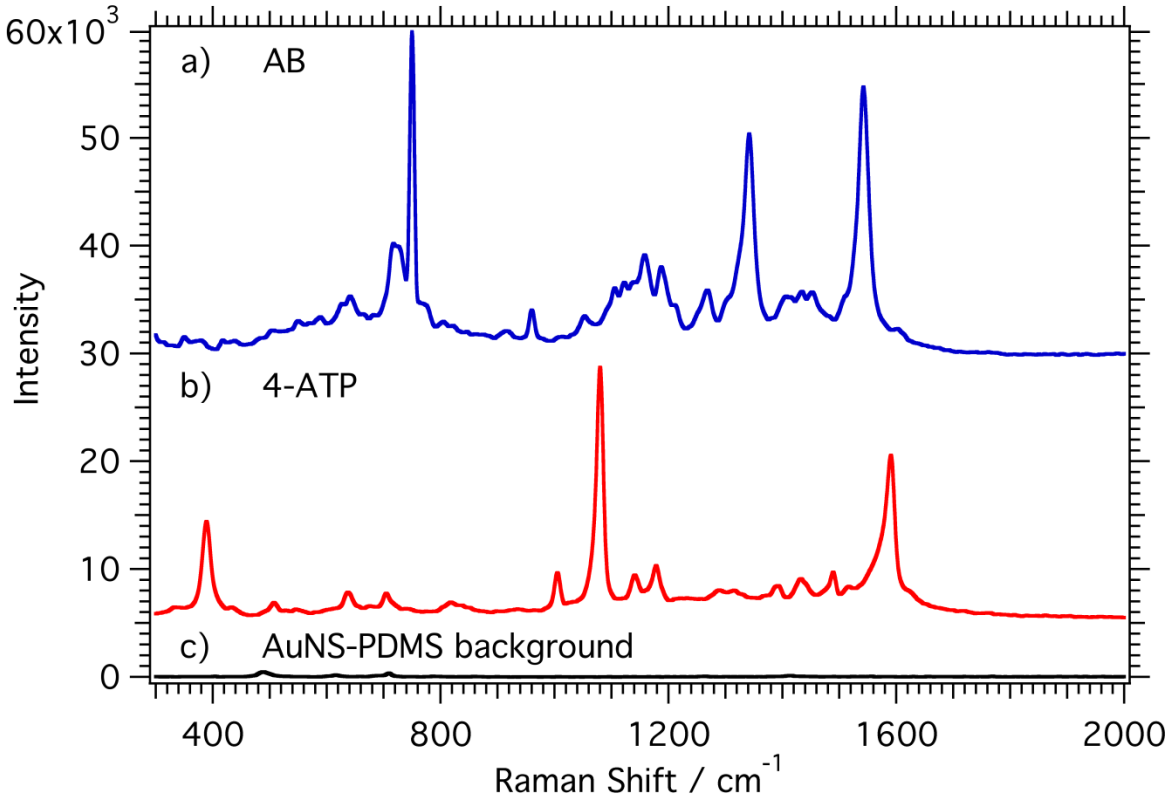

Figure S5: SERS spectra of a) astra blue ([AB]=10^{-7} M) and b) 4-ATP ([4-ATP]=10^{-6} M) on PDMS slides functionalized with PVP coated Au nanostars, recorded at a laser wavelength of 785 nm, with power of 1 mW and 10 s exposition time. c) Collected background under the same conditions in the absence of the analyte molecules. Both SERS spectra are background corrected and an offset was applied to improve the differentiation of spectra.

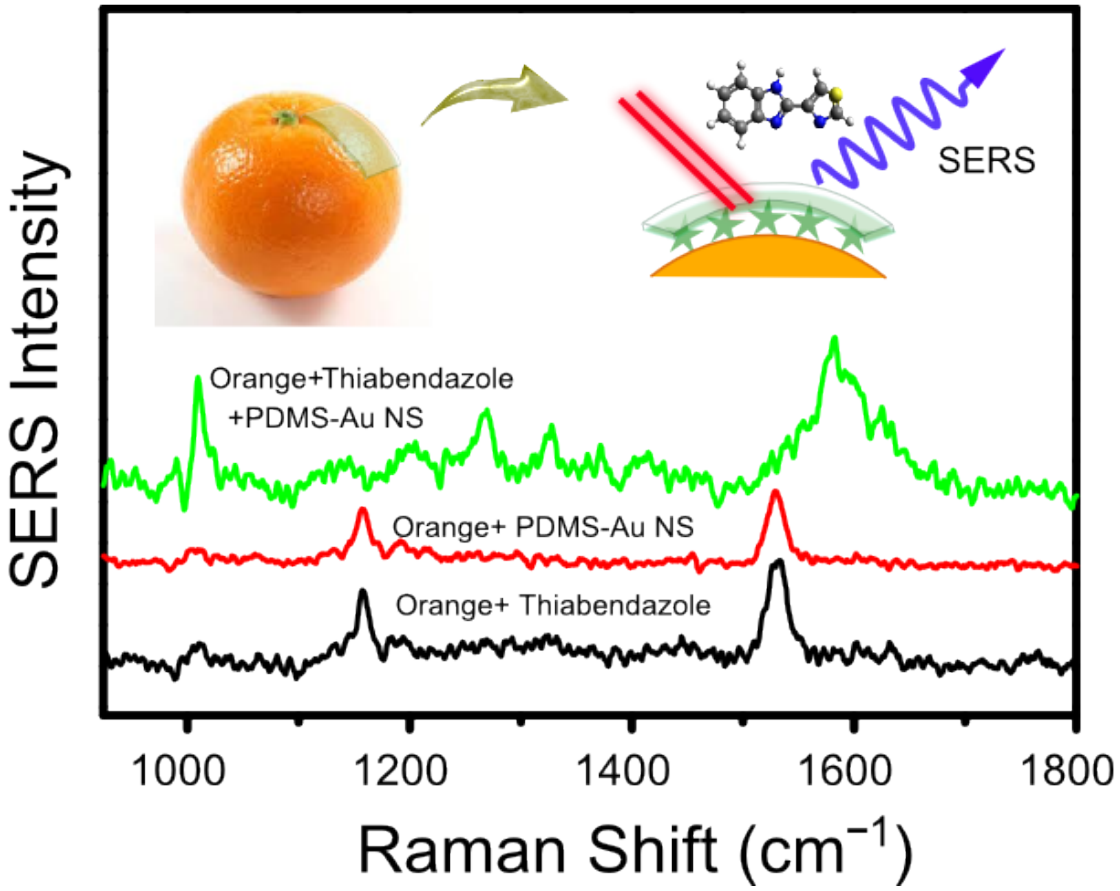

Figure S6: SERS spectrum of thiabendazole adsorbed on orange skin, acquired by covering the orange skin with Au NS/PDMS substrate and then excited from the backside of the substrate with 785 nm laser. Two control spectra are shown, which were obtained from the same orange skin with pesticide but without enhancing substrate; and by covering a clean orange skin with Au NS/PDMS substrate. The presence of pesticide can be clearly distinguished as the spectrum is completely different from the background in the presence of pesticide and the corresponding Raman bands can be clearly distinguished (phenyl ring breathing mode at 1008 cm^{-1}, skeletal ring C-N, C=N-N stretch at 1270 cm^{-1} and skeletal ring stretching mode at 1576 cm^{-1}).